



Published in final edited form as:

*J Alzheimers Dis.* 2019 ; 67(1): 393–410. doi:10.3233/JAD-180941.

## Acidifying endolysosomes prevented LDL-induced amyloidogenesis

Liang Hui, Mahmoud L. Soliman, Nicholas H. Geiger, Nicole M. Miller, Zahra Afghah, Koffi L. Lakpa, Xuesong Chen\*, and Jonathan D. Geiger

Department of Biomedical Sciences, University of North Dakota School of Medicine and Health Sciences, Grand Forks, ND 58203, USA

### Abstract

Cholesterol dyshomeostasis has been linked to the pathogenesis of sporadic Alzheimer's disease (AD). In furthering the understanding of mechanisms by which increased levels of circulating cholesterol augments the risk of developing sporadic AD, others and we have reported that LDL enters brain parenchyma by disrupting the blood-brain barrier and that endolysosome de-acidification plays a role in LDL-induced amyloidogenesis in neurons. Here, we tested the hypothesis that endolysosome de-acidification was central to amyloid beta (A $\beta$ ) generation and that acidifying endolysosomes protects against LDL-induced increases in A $\beta$  levels in neurons. We demonstrated that LDL, but not HDL, de-acidified endolysosomes and increased intraneuronal and secreted levels of A $\beta$ . ML-SA1, an agonist of endolysosome-resident TRPML1 channels, acidified endolysosomes, and TRPML1 knockdown attenuated ML-SA1-induced endolysosome acidification. ML-SA1 blocked LDL-induced increases in intraneuronal and secreted levels of A $\beta$  as well as A $\beta$  accumulation in endolysosomes, prevented BACE1 accumulation in endolysosomes, and decreased BACE1 activity levels. LDL down regulated TRPML1 protein levels, and TRPML1 knockdown worsens LDL-induced increases in A $\beta$ . Our findings suggest that endolysosome acidification by activating TRPML1 may represent a protective strategy against sporadic AD.

### Keywords

LDL; cholesterol; amyloid beta; BACE1; endolysosome pH; ML-SA1; TRPML1; neurons

### Introduction

Alzheimer's disease (AD) is a devastating neurodegenerative disorder that is characterized clinically by progressive impairments in memory and cognition, and neuropathologically by loss of synaptic integrity, accumulations of amyloid beta (A $\beta$ ) and phosphorylated tau proteins, and increased levels of oxidative stress [1–4]. A $\beta$  continues to be considered an important pathogenic factor of AD [5, 6], and mutations in A $\beta$  precursor protein (A $\beta$ PP) and

\*Address Correspondence to: Xuesong Chen, MD, Ph.D., Assistant Professor, Department of Biomedical Sciences, University of North Dakota School of Medicine and Health Sciences, 504 Hamline Street, Grand Forks, North Dakota 58203, (701) 777-0919, xuesong.chen@med.und.edu.

Conflict of Interest/Disclosure Statement

The authors have no conflict of interest to report.

presenilin proteins result in early-onset familial AD [5]. However, the vast majority of AD cases are sporadic in nature.

Currently, pathogenic mechanisms responsible for the accumulation of A $\beta$  in sporadic AD remain unclear, but are believed to result from complex interactions between aging, nutritional, environmental and genetic factors [7]. Among these factors, altered levels of circulating cholesterol have been implicated in the pathogenesis of sporadic AD [8–12]. More specifically, as the single strongest genetic risk factor for sporadic AD [7, 13], ApoE4 is clearly associated with elevated plasma levels of low-density lipoprotein (LDL) and decreased levels of high density lipoprotein (HDL) [14, 15]; High levels of plasma LDL, independent of APOE genotypes, increase the risk of developing sporadic AD [8, 11, 16–20]; And low levels of plasma HDL, independent of the APOE genotype, are associated with decreased risk of developing AD [11, 19, 21, 22].

How altered circulating cholesterol contributes to the pathogenesis of sporadic AD in brain remains unclear, especially when essentially all brain cholesterol is locally synthesized and there is no exchange of LDL particles across an intact blood-brain barrier (BBB) [23]. As such, apoB-100, the exclusive LDL carrier protein in circulating blood, is not present in normal brain [24]. However, under conditions when the BBB is compromised, as occurs early in sporadic AD [25–30], plasma LDL can enter brain parenchyma where it may contribute to the pathogenesis of sporadic AD. In support, impairment of the BBB can increase cholesterol flux from the peripheral circulation into brain [31], and apoB-100 is present in AD brain, where it has been shown to co-localize with A $\beta$  [9, 24, 32–34]. In addition, others and we have shown that high levels of plasma cholesterol disrupts the BBB [35–37] and increases brain levels of apoB-100 [9, 38]. Thus, circulating LDL, when entering brain parenchyma through a compromised BBB, could have a direct effect on the development of AD in brain.

In brain, LDL can be internalized into endolysosomes via receptor-mediated endocytosis, and thus LDL could directly disturb endolysosome function. Consistent with findings that endolysosome dysfunction is an early and prominent pathological feature in sporadic AD [39, 40], we have shown that LDL de-acidifies neuronal endolysosomes, induces endolysosome dysfunction, and enhances amyloidogenic processing of A $\beta$ PP in endolysosomes [10]. Because endolysosome de-acidification in neurons appears to play an important role in LDL-induced amyloidogenesis, it is likely that endolysosome acidification may decrease the pathogenesis of AD [41].

Here, we compared the effects of LDL and HDL on endolysosome function and A $\beta$  generation in neurons. We also determined the extent to which and mechanisms by which ML-SA1, an agonist of endolysosome TRPML1 channels, affects endolysosome pH and LDL-induced increases in A $\beta$  generation in neurons. We demonstrated that LDL, but not HDL, de-acidified endolysosomes and increased A $\beta$ . Furthermore, we found that ML-SA1 acidified endolysosomes and prevented LDL-induced endolysosome de-acidification and increases in A $\beta$  levels. Mechanistically, we demonstrated that TRPML1 channels were specifically involved in the endolysosome acidifying effects of ML-SA1 and its protective effects on LDL-induced amyloidogenesis.

## Material and Methods

### Cells:

Primary cultures of cortical neurons were prepared from embryonic day 18 Sprague-Dawley rats using a protocol approved by the University of North Dakota Animal Care and Use Committee adherent with the Guide for the Care and Use of Laboratory Animals (NIH publication number 80–23). Pregnant dams (embryonic day 18) were sacrificed by asphyxiation with CO<sub>2</sub>. The fetuses were removed, decapitated, and meninges-free cerebral cortices were isolated, trypsinized, and plated onto 35-mm poly-D-lysine-coated glass-bottom tissue culture dishes. Neurons were grown in Neurobasal™ medium with L-glutamine, antibiotic/antimycotic and B<sub>27</sub> supplement, and were maintained at 37°C and 5% CO<sub>2</sub>. Typically, the purity of the neuronal cultures was greater than 95% as determined by immunostaining with neuronal (mouse anti-NeuN, Millipore MAB377 or Chicken anti-MAP2 antibodies, Millipore AB15452) and astrocyte (mouse anti-GFAP antibody, Sigma, G3893) markers. Neuron were kept in culture for 10–14 days, at which time they were treated with LDL (Kalen Biomedical) or HDL (Kalen Biomedical) for another 3 days. Human neuroblastoma cells (SH-SY5Y) expressing wild type AβPP were kindly supplied by Dr. Norman Haughey (John Hopkins University).

SH-SY5Y cells were cultured in Eagle's minimum essential medium (MEM) supplemented with 10% FCS, penicillin/streptomycin, nonessential amino acids, and sodium pyruvate (1 mM) at 37°C in 5% CO<sub>2</sub>. For our experiments, 4 × 10<sup>6</sup> SH-SY5Y cells were seeded on 60 mm<sup>2</sup> dishes and cultured for 48 h at which time the media was changed to serum-free MEM and treated with LDL (Kalen Biomedical) or HDL (Kalen Biomedical) for 3 days. ApoB from human plasma (Sigma, A5353) and recombinant human apoE3 (Sigma, SRP4696) were used to prepare the mixture of HDL/apoB and HDL/apoE3.

### Measurement of endolysosome pH:

Endolysosome pH was measured using a ratio-metric lysosome pH indicator dye (LysoSensor Yellow/Blue DND-160, Invitrogen); a dual excitation dye that permits pH measurements in acidic organelles independently of dye concentration. Neurons were loaded with LysoSensor (2 μM) for 5 minutes at 37°C. Light emitted at 520 nm in response to excitation at 340 nm and 380 nm was measured for 20 ms every 5 seconds using a filter-based imaging system (Zeiss and 3i). The ratios of light excited at 340/380 nm and emitted at 520 nm were converted to pH using a calibration curve established using 10 μM of the H<sup>+</sup>/Na<sup>+</sup> ionophore monensin, and 20 μM of the H<sup>+</sup>/K<sup>+</sup> ionophore nigericin dissolved in 20 mM 2-(N-morpholino) ethane sulfonic acid (MES), 110 mM KCl, and 20 mM NaCl adjusted to pH 3.0 to 7.0 with HCl/NaOH.

### Lysosome fraction preparation:

Crude lysosome fractions were prepared using a lysosome isolation kit (Sigma). Cells were homogenized in extraction buffer, and homogenates were centrifuged at 1,000 × g for 10 minutes at 4°C. Supernatants were collected and pellets were homogenized in 2 volumes of 1× extraction buffer and centrifuged at 1,000 × g for 10 minutes at 4°C. The two supernatants were pooled and then centrifuged at 20,000 × g for 20 minutes at 4°C. Pellets

were resuspended in 0.5 ml of 1× extraction buffer and this fraction contained a mixture of light mitochondria, endosomes, lysosomes, peroxisomes, and endoplasmic reticulum.

#### Measurement of BACE1 activities:

BACE1 activity was determined using 50 mM synthetic peptide substrates containing the BACE1 cleavage site (MCA-Glu-Val-Lys-Met-Asp-Ala-Glu-Phe-(Lys-DNP)-OH) (Calbiochem). Equal amounts of protein (50 µg) were used from each sample lysate. The fluorescence was measured using a fluorescence microplate reader with an excitation wavelength set at 320 nm and an emission wavelength set at 383 nm. As a control for specificity, BACE1 activity was tested in the absence and presence of the BACE-1 inhibitor, H-Lys-Thr-Glu-Glu-Ile-Ser-Glu-Val-Asn-Stat-Val-Ala-Glu-Phe-OH (Calbiochem).

#### Immunoblotting:

Cells were lysed with RIPA buffer (Pierce) plus 10 mM NaF, 1 mM Na<sub>3</sub>VO<sub>4</sub> and Protease Inhibitor Cocktail (Sigma). After centrifugation (14,000 × g for 10 min at 4°C), supernatants were collected, and protein concentrations were determined with a DC protein assay (Bio-Rad). Proteins (10 µg) were separated by SDS-PAGE (12% gel) and transfer to polyvinylidene difluoride membranes (Millipore). The membranes were incubated overnight at 4°C with antibodies against acid phosphatase (Abcam, ab58688), TRPML1 (Sigma, HPA031763), N-terminal AβPP (Thermofisher, 14-9749-80), BACE-1 (Thermofisher, MA1-177), LAMP-1 (Sigma, L1418), v-ATPase V1A1 (Santa Cruz, sc-374475), v-ATPase V0a1 (Thermofisher, PA5-69418). GAPDH (Abcam, ab8245) was used as a gel loading control. The blots were developed with enhanced chemiluminescence, and bands were visualized and analyzed using our Odyssey<sup>Fc</sup> multi-modal imager system (Li-Cor). Quantification of results was performed by densitometry and the results were analyzed as total integrated densitometric volume values (arbitrary units).

#### Immunostaining:

Cells were fixed with cold methanol (−20°C) for 10 min, washed with PBS, blocked with 5% goat serum, and incubated overnight at 4°C with primary antibodies including amyloid beta mouse antibody MOAB-2 (Biosensis, M-1586), BACE1 mouse antibody (Thermofisher, MA1-177) and lysosome-associated membrane protein-1 (LAMP1) rabbit antibody (Sigma, L1418). After washing with PBS, cells were incubated with fluorescence-conjugated secondary antibodies including Alexa 488-conjugated goat anti-mouse antibody (Invitrogen) and Alexa 546-conjugated goat anti-rabbit antibody (Invitrogen). Images were taken using our confocal microscope (Zeiss 800). Controls for specificity included staining with primary antibodies without fluorescence-conjugated secondary antibodies (background controls) and staining with only secondary antibodies; these controls eliminated auto-fluorescence in each channel and bleed-through (crossover) between channels. Averaged fluorescent intensities per cell was quantified using Image J software (NIH). Percentage of colocalization were quantified using Image J software (NIH) and data were normalized to control.

### Quantification of A $\beta$ levels:

Secreted and intracellular A $\beta$  levels were measured using human/rat A $\beta$ 1–40 and A $\beta$ 1–42 ELISA kits (Wako). For secreted A $\beta$  measurements, media from cultured cells was collected, diluted 1:4 with standard diluent buffer, and each sample was analyzed in duplicate. Total cellular protein levels were determined by a DC protein assay (Bio-Rad). A $\beta$  levels were normalized to total protein content in each sample. For intracellular A $\beta$  measurements, cells were diluted 8-times (w/v) with ice-cold 5 M guanidine-HCl/50 mM Tris-HCl cells and were homogenized. The homogenates were diluted with ice-cold reaction buffer (Dulbecco's phosphate-buffered saline containing 5% BSA and 0.03% Tween-20 supplemented with 1 $\times$  protease inhibitor cocktail). Following centrifugation at 16,000  $\times$  g for 20 min at 4°C, supernatants were collected, diluted 1:1 with standard diluent buffer, and quantified by colorimetric sandwich A $\beta$  ELISA kits (Wako). Intracellular A $\beta$  levels were normalized to total protein content in the samples.

### RNA interference:

TRPML1 (mucolipin1) protein levels were knocked down with specific rat siRNAs (RSS305451, RSS305452, RSS305453 from ThermoFisher) at a final concentration of 20 nM; negative siRNAs (4404020 from ThermoFisher) were used as controls. Before siRNA transfection, fresh Neurobasal media was added to cultured neurons plated for 10 days. The transfection cocktail containing transfection buffer (SignaGen), TRPML1 siRNA stock, and GenMute™ reagent was added carefully to each dish along with fresh Neurobasal media. After incubation (37°C, 5% CO<sub>2</sub>) for 5 h, the transfection media was replaced with fresh Neurobasal media or treated with LDL for another 48 hours. Knockdown efficiency was measured by immunoblotting.

### Statistical analysis:

All data were expressed as means and SEM. Statistical significance for multiple comparisons was determined by one-way ANOVA plus a Tukey post-hoc test or by Student's t-test.  $p < 0.05$  was considered to be statistically significant.

## Results

### LDL, but not HDL, increases A $\beta$ .

Given epidemiological findings that LDL increases, whereas HDL decreases, the risk of developing AD, we first determined the extent to which LDL and HDL affects intraneuronal and secreted levels of A $\beta$ . It should be noted that there is a species difference in the composition of lipoproteins. Human liver produces only apoB100, whereas rodent liver produces a mixture of ApoB100 and ApoB48 [42]. Thus, human LDL particles contain only apoB100, whereas rodent LDL particle contains both apoB100 (slightly dominating) and apoB48. Because apoB48 lacks the canonical LDLR binding site, human LDL particles and rodent LDL particles exhibit different receptor binding property [43]. Rodent HDL particles is also different from that of humans. ApoE is the major protein component of rodent HDL, whereas human HDL contain only small amounts of apoE. Thus, in rodents, HDL particles are the predominant class of lipoproteins that transport plasma cholesterol; but in humans,

LDL particles are the major transporter of plasma cholesterol [43]. Due to these differences in lipoproteins and lipid profiles, rodents are relatively resistant to the development of atherosclerosis. For these reasons, LDL and HDL derived from human plasma are used in the present study. In SH-SY5Y cells, LDL treatment (50  $\mu\text{g}/\text{ml}$  for 3 days) significantly increased secreted levels of  $\text{A}\beta_{1-40}$  and  $\text{A}\beta_{1-42}$  (Figure 1A), and intraneuronal levels of  $\text{A}\beta_{1-40}$  and  $\text{A}\beta_{1-42}$  (Figure 1B). However, HDL treatment (50  $\mu\text{g}/\text{ml}$  for 3 days) did not significantly increase secreted or intraneuronal levels of  $\text{A}\beta$ . In contrast to LDL, HDL decreased significantly secreted levels of  $\text{A}\beta_{1-40}$  (Figure 1A). Neither LDL nor HDL affected protein levels of full-length  $\text{A}\beta\text{PP}$  (Figure 1C), but LDL (not HDL) increased protein levels of BACE1 (Figure 1D). At the concentrations used, neither LDL nor HDL induced significant levels of cell death as indicated by LDH releasing assay (data not shown). To determine whether LDL-induced increases in  $\text{A}\beta$  is due to increased cell proliferation, we measured total protein levels in cells treated with LDL and HDL for 3 days as compared with cells without any treatment for 3 days (control). We found that total cellular protein concentrations ( $\mu\text{g}/\mu\text{l}$ ) following treatment with LDL ( $0.37\pm 0.13$ ), HDL ( $0.31\pm 0.03$ ), or control ( $0.34\pm 0.04$ ) were not different ( $n=5$ ,  $p>0.05$ ). Given that cells were seeded at the same density at the beginning of treatment and total cellular proteins were collected in the same way, our finding suggests that LDL does not affect cell proliferation when compared with HDL.

Because apoB, the exclusive apolipoprotein of LDL, is not present in plasma HDL or in brain in situ synthesized apoE-rich lipoprotein, we then determined the effect of HDL mixed with apoB or apoE3 on the production of  $\text{A}\beta$  in SH-SY5Y cells. ApoE-rich lipoproteins synthesized *in situ* in brain is thought to be HDL-like particles composed of phospholipids and un-esterified cholesterol [44–46]. To model brain in situ apoE-rich HDL-like lipoproteins, we pre-incubated apoE3 with HDL with a fixed ratio of 0.4 for apoE protein/HDL protein. This ratio was based on findings that the phospholipid content of human plasma HDL is about 29% and the protein content of human plasma HDL is about 40%; thus, the ratio of phospholipids/protein content of HDL is about 0.7 [47]. Furthermore, the apoE/phospholipid ratio in CSF is about 0.6 [48]. Therefore, if one assumes that the phospholipid (HDL) content is similar in plasma and CSF, the calculated ratio of apoE protein/HDL protein content in CSF is 0.42. Similarly, we pre-incubated apoB with HDL with a fixed ratio of 0.4 for apoB protein/HDL protein. We demonstrated that treatment with HDL (50  $\mu\text{g}/\text{ml}$ ) mixed with apoB (20  $\mu\text{g}/\text{ml}$ ) for 3 days significantly increased secreted levels of  $\text{A}\beta_{1-40}$  and  $\text{A}\beta_{1-42}$  (Figure 2A) and intraneuronal levels of  $\text{A}\beta_{1-40}$  and  $\text{A}\beta_{1-42}$  (Figure 2B). However, treatment with HDL (50  $\mu\text{g}/\text{ml}$ ) mixed with apoE3 (20  $\mu\text{g}/\text{ml}$ ) for 3 days did not significantly increase secreted or intraneuronal levels of  $\text{A}\beta$  (Figure 2).

### **LDL, but not HDL, de-acidified endolysosomes.**

Amyloidogenic processing of  $\text{A}\beta\text{PP}$  occurs predominantly in endosomes where the acidic pH is compatible with high levels of BACE1 expression and activity [49, 50]. Thus, we determined the extent to which LDL and HDL affect endolysosome pH in SH-SY5Y cells. We found that LDL (50  $\mu\text{g}/\text{ml}$  for 3 days), but not HDL (50  $\mu\text{g}/\text{ml}$  for 3 days), increased significantly endolysosome pH (Figure 3A). Because v-ATPase is the main proton pump that maintains the acidic environment of endolysosomes, we then determined the extent to which



LDL and HDL affected total levels and endolysosomal protein levels of v-ATPase. We found that LDL, but not HDL, significantly decreased total protein levels of v-ATPase V1A1 and V0a1 subunits in whole cell lysates (Figure 3B). Furthermore, LDL, but not HDL, significantly decreased protein levels of v-ATPase V1A1 and V0a1 subunits in enriched lysosome fractions (Figure 3C).

#### **ML-SA1 acidified endolysosomes.**

The above findings suggest that endolysosome deacidification plays a role in LDL-induced increases in A $\beta$ . To further determine a cause role of endolysosome deacidification in LDL-induced increases in A $\beta$ , we need an agent that could acidifies endolysosomes. Given that activating TRPML1 channels with ML-SA1 has been shown to reduce endolysosome cholesterol accumulation in Niemann–Pick’s disease type C [51], we determine the extent to which ML-SA1 affects endolysosome pH in rat primary cultured neurons. We found that ML-SA1 (20  $\mu$ M) decreased acutely endolysosome pH in neurons (Figure 4A). Given that ML-SA1 is an agonist of TRPML1, we determined if TRPML1 was involved in the endolysosome acidifying effects of ML-SA. Thus, we knockdown the expression of TRPML1 using siRNA in primary cultured neurons (Figure 4B). We found that TRPML1 knockdown did not affect basal levels of endolysosome pH; however, TRPML1 knockdown blocked significantly the magnitude of ML-SA1-induced acidification of endolysosomes (Figure 4C). These findings indicate that ML-SA1 induced endolysosome acidification is, at least, in part by activating TRPML1.

#### **ML-SA1 prevented LDL-induced increases in A $\beta$ .**

Consistent with findings described above using SH-SY5Y cells, we demonstrated in primary cultured rat cortical neurons that LDL (50  $\mu$ g/ml for 3 days) increased secreted levels of A $\beta$ <sub>1–40</sub> (Figure 5A) and A $\beta$ <sub>1–42</sub> (Figure 5B). Importantly, ML-SA1 (20  $\mu$ M) co-treatment decreased significantly basal level of secreted A $\beta$  and blocked significantly LDL-induced increases in secreted levels of A $\beta$ <sub>1–40</sub> (Figure 5A) and A $\beta$ <sub>1–42</sub> (Figure 5B). Using an antibody (MOAB-2) specific to A $\beta$  (residues 1–4) that is capable of differentiating A $\beta$  from A $\beta$ PP [52] and an antibody targeting lysosome-associated membrane protein 1 (LAMP1), we then determined the effects of LDL and ML-SA1 on endolysosome accumulation of A $\beta$ . We demonstrated that LDL increased significantly immunopositive signals of A $\beta$  (Figure 5C, D) and increased the co-localization of A $\beta$  with LAMP1 positive lysosome (Figure 5E), and that such effects were prevented by ML-SA1 (Figure 5C, D, E). In addition, we found that LDL treatment has changed the distribution of LAMP1-positive vesicles. In control neurons, LAMP1-positive endolysosomes were relatively small and homogeneous in size and were distributed primarily in axon hillock region. However, in neurons treated with LDL, LAMP1-positive signals were increased, LAMP1-positive endolysosomes were markedly enlarged, often clumped together, and distributed throughout neuron soma (Figure 5C).

Given that BACE1 is the critical enzyme for A $\beta$  generation, we further determined the extent to which LDL and ML-SA1 affect BACE1. We found that LDL (50  $\mu$ g/ml for 3 days) increased immunopositive signals of BACE1 and increased co-localization of BACE1 with LAMP1 positive lysosomes, and that such effect were prevented by ML-SA1 (Figure 6A, B). In addition, LDL treatment changed the sizes and the distribution of LAMP1-positive

endolysosomes similar to those observed in Figure 5. Furthermore, LDL (50  $\mu\text{g/ml}$  for 3 days) increased significantly BACE1 activity, an effect that was blocked by ML-SA1 (Figure 6C).

### TRPML1 knockdown potentiated LDL-induced increases in A $\beta$ .

Given that TRPML1 is involved in ML-SA1-induced endolysosome acidification and that LDL de-acidifies endolysosomes, we determine if LDL treatment could affect TRPML1 protein levels. We demonstrated that LDL (50  $\mu\text{g/ml}$  for 3 days) significantly decreased protein levels of TRPML1 in neurons (Figure 7A). Next, we determined the extent to which siRNA knockdown of TRPML1 (Figure 4B) affected LDL-induced increases in A $\beta$ . We found that TRPML1 knockdown, per se, did not affect secreted levels of A $\beta_{1-40}$  or A $\beta_{1-42}$ ; however, TRPML1 knockdown significantly exacerbated LDL-induced increases in secreted levels of A $\beta_{1-40}$  and A $\beta_{1-42}$  (Figure 7B).

## Discussion

Dyshomeostasis of circulating levels of cholesterol have been implicated in the pathogenesis of sporadic AD [8–12, 19, 21, 22]. Our studies here were focused to determine specifically how LDL-induced endolysosome de-acidification increased A $\beta$  levels in neurons and to elucidate mechanisms by which endolysosome acidification protected against LDL-induced increases in A $\beta$  levels. The main findings were (1) that LDL, but not HDL, de-acidified endolysosomes and increased intracellular and secreted levels of A $\beta$ , (2) that TRPML1 was responsible for the endolysosome acidifying effects of ML-SA1, (3) that acidifying endolysosomes with ML-SA1 prevented LDL-induced increases in A $\beta$ , and (4) that LDL decreased protein levels of TRPML1 and TRPML1 knockdown worsened LDL-induced increases in A $\beta$ . Thus, acidification of endolysosomes by activating TRPML1 might be targeted for new therapeutic strategies against sporadic AD.

Altered cholesterol homeostasis, independent of APOE genotypes, has been linked to the pathogenesis of sporadic AD. However, it is not fully understood how cholesterol dyshomeostasis in circulating blood contributes to the development of AD in brain. Whether synthesized in the periphery or in brain, cholesterol is the same; however, lipoproteins associated with cholesterol differ in size, lipid composition, and mechanisms governing their transport and uptake. In plasma, LDL is the main lipoprotein particle that mediates the transport of cholesterol and lipids into periphery tissues, whereas HDL is the lipoprotein particle that mediates the reverse - cholesterol efflux from periphery tissues. LDL is a 20–25 nm sized particle that has the highest cholesterol content, and apoB-100, which is exposed at the surface of LDL allowing receptor recognition, is the exclusive apolipoprotein that mediates LDL transport and uptake. LDL particles constitute 90% of circulating apoB-containing lipoproteins, with each LDL particle containing a single apoB-100 molecule. HDL, a protein-rich disc-shaped particles, is about 8–10 nm in size, has lower cholesterol content, and primary apolipoproteins that mediate its transport and uptake are apoA-I, apoC-I, apoC-II and apoE. In brain, apoE-rich HDL-like lipoproteins mediates that transport of cholesterol and lipids. Under normal conditions, the intact BBB restricts plasma LDL from entering brain parenchyma and brain cholesterol is almost completely dependent on *in situ*



synthesis of apoE-containing cholesterol by astrocytes [53]. Although the intact BBB restricts prevent LDL particle from entering brain parenchyma, a small apoB peptide (receptor binding domain of apoB) has been shown to function as a BBB shuttle peptide without affecting the BBB integrity [54]. Unlike LDL, a small fraction of circulating HDL can enter the brain even with an intact BBB, and it has been shown that HDL has largely protective effects [55, 56]. Consistent with the reported protective role of HDL, we showed here that HDL could decrease secreted levels of A $\beta$ .

Complex interactions between aging, nutritional, environmental and genetic factors contribute to the development of sporadic AD [7]. Among these factors, vascular risk factors play a significant role in the development and progression of AD [57–59]. Increased plasma levels of LDL, which is present in many vascular risk factors, including atherosclerosis, hypertension, diabetes, and obesity, is directly implicated in the development of atherosclerotic cardiovascular disease [60]. Increased plasma levels of LDL, as well as, various vascular risk factors have been implicated to the breakdown of the BBB [57, 61, 62]. Indeed, recent advanced neuroimaging studies have shown BBB breakdown in discrete brain regions of individual with mild cognitive impairment and early AD [63–66]. In addition, high prevalence of cerebral microbleeds are detected individuals with mild cognitive impairment and early AD [67–69], and these cerebral microbleeds correlate to the distribution of A $\beta$  deposition [70]. Furthermore, pathological features of BBB breakdown, such as loss of tight junctions and extravasation of blood-derived proteins, have been confirmed in postmortem AD brains [71]. Although not all AD patients have uniform BBB breakdown, BBB integrity is compromised early in the pathogenesis of AD and precedes the apparent brain deposition of A $\beta$  [26].

Under conditions when BBB integrity is compromised as occurs early in AD, a significant amount of cholesterol could flux from circulation into the brain parenchyma [31]. Indeed, as the exclusive apolipoprotein of circulating LDL, apoB100 is present in AD brain [32], where it co-localizes with A $\beta$  in human AD brain and in animal models [19, 32, 33, 72]. The presence of apoB-100 in AD brain could be due to the leakage of apoB-containing LDL particles into the brain or just the leakage of ApoB into the brain. Although LDL are large particles (about 20–25 nm in size and molecular mass ranging from 2.4 to 3.9MDa), under conditions when BBB is severely damaged as occurs with microbleeds [73], LDL particles could enter brain parenchyma. Once entering brain, apoB-containing LDL cholesterol can be internalized by neurons via receptor-mediated endocytosis with the assistance of highly expressed receptors for cholesterol uptake. Because apoB and apoE have different affinities for receptors for cholesterol uptake, neuronal uptake of apoB-containing LDL may result in drastic difference in intracellular cholesterol transport and distribution than that of apoE cholesterol. In support, it has been shown that apoB leads to cholesterol being targeted by the lysosome degradation pathway [74, 75], whereas apoE mediates cholesterol recycling [76–78]. Thus, neuronal uptake of apoB-containing LDL cholesterol could lead to cholesterol accumulation in endolysosomes [10]. Consistently, we have shown that accumulation of apoB100 and cholesterol in endolysosomes in brain of a rabbit model of sporadic AD [38, 79]. Thus, apoB-containing LDL could directly contribute to the disturbances of neuronal endolysosome structure and function - another early pathological features of sporadic AD [80, 81].

Given that highly acidic pH is critical for essential for regulating many functions of endolysosomes, the simplest explanation for the observed pathological changes of endolysosomes in post-mortem brain tissue from AD patients [80–82] is that endolysosome pH is de-acidified both in familial AD and in sporadic AD. In familial AD, presenilin 1 mutation has been shown to result in endolysosome de-acidification [83, 84], while familial AD-mutant APP over-expression may lead to a deficit in endolysosome de-acidification as implicated by endolysosomal dysfunction [85, 86]. In sporadic AD, endolysosome de-acidification may result from complex interactions between aging and environmental factors. Age-dependent lipofuscin accumulation may act as v-ATPase inhibitors and promote endolysosomal de-acidification [87], chronic oxidative stress results from aging and environmental factors may impair v-ATPase and lead to deficit in endolysosome acidification [88, 89], and lipid accumulation [90, 91] and iron overload [92–94] in endolysosome may also de-acidify endolysosomes. Consistently, we have shown that following its endocytosis into and accumulation by endolysosomes [95], apoB-containing LDL de-acidifies endolysosomes in both primary neuron and in SH-SY5Y cells. These findings provide further mechanistic insights on how cholesterol dyshomeostasis in circulating blood contributes to the development of AD in brain.

It is well known that endolysosomes play a central role in A $\beta$  production and metabolism [81, 96]. Amyloidogenic processing of A $\beta$ PP predominantly occurs in endosomes, where the pH is optimum BACE1 activity [49, 50], and such endosome-derived A $\beta$  can be further degraded by cathepsin D in more acidic lysosomes [97–100]. Thus, simply altering endolysosome pH could have a profound effect on proteolytic A $\beta$ PP processing in endolysosomes and A $\beta$  levels. In support, chloroquine, a known weak base that neutralize the acidic pH in endolysosomes, has been shown to induce accumulation of lipids [101, 102] and A $\beta$ PP by-products in endolysosomes [103] and increase A $\beta$  levels [104, 105]. Similarly, bafilomycin, a known v-ATPase inhibitor, has also been shown to increase A $\beta$  levels [106]. It is interesting to note that these two known alkalizing agents increase A $\beta$  levels in wild-type A $\beta$ PP expressing cells; however, they decrease A $\beta$  levels in Swedish-mutation A $\beta$ PP expressing cells [104, 106, 107]. Currently, it is not understood what leads to such a discrepancy. In addition, U18666A, an agent that leads to cholesterol accumulation in endolysosomes, de-acidifies endolysosomes [108], and increases A $\beta$  levels [109]. On the other hand, restoring endolysosomal acidification by GSK3 inhibition [110] or acidic nanoparticle [111–113] has been shown to improve amyloid pathology.

Because the activity of BACE-1 is optimal at a pH  $\approx$  5 [114, 115] and is degraded in lysosomes at a pH  $\approx$  4 [116] and because the activity of cathepsin D is optimal at a pH  $\approx$  3.5 [117], subtle de-acidification could shift lysosomes into an endosome phenotype to increase A $\beta$  production and impair A $\beta$  lysosome degradation, whereas subtle acidification could shift endosome into lysosome phenotype to decrease A $\beta$  generation and enhance A $\beta$  lysosome degradation. In the present study, LDL-induced slight increases in endolysosome pH could have resulted in decreased degradation of BACE-1 and increased accumulation and activity of BACE-1 in endolysosomes (Figure 6), thus increasing A $\beta$  production. On the other hand, LDL-induced increases in endolysosome pH could have resulted in inhibition of cathepsin D activity [95], thus impairing the degradation of A $\beta$  in lysosomes and increasing A $\beta$  accumulation in lysosomes (Figure 5). The above scenario might have occurred when

endolysosome is mildly alkalized as induced by LDL treatment. Under conditions when the acidic environment of endolysosomes is severely impaired, the drastic alkalization could block proteolytic processing A $\beta$ PP, leading to accumulation of full-length A $\beta$ PP in endolysosomes [118] and decreased A $\beta$  levels. The centrality of endolysosome pH in LDL-induced amyloidogenesis in neurons is further strengthened by our findings that ML-SA1 acidifies endolysosomes and blocks LDL-induced increases in BACE-1 activity and A $\beta$  levels. The mild acidification induced by ML-SA1 could block LDL-induced impaired degradation of BACE-1 and increased accumulation and activity of BACE-1 in endolysosomes, thus preventing LDL-induced increasing A $\beta$  production. On the other hand, the mild acidification induced by ML-SA1 could block LDL-induced inhibition of cathepsin D activity [95], thus preventing LDL-induced impairment in the degradation of A $\beta$  in lysosomes and increased A $\beta$  accumulation in lysosomes.

We demonstrated that the endolysosome acidifying effects of ML-SA1 is, at least in part, dependent on the activation of endolysosome-resident TRPML1 cation channels. Although the mechanisms by which TRPML1 activation affects endolysosome pH are unclear it is possible that calcium released from TRPML1 activates calcium-activated potassium channels and increases an exchange of potassium and hydrogen ions [119–121]. Alternatively, calcium released from TRPML1 might affect the activity of v-ATPase, the key proton pump that maintains the acidic environment of endolysosomes. Finally, the endolysosome de-acidifying effects of LDL could be linked directly to TRPML1 because LDL decreases protein levels of TRPML1 and TRPML1 activation has been shown to activate v-ATPase [122]. Regardless of the mechanism, our findings suggest that endolysosome de-acidification plays a critical role in LDL-induced amyloidogenesis and that endolysosome acidification by activating TRPML1 might represent a therapeutic strategy against AD.

## Acknowledgments

We greatly acknowledge the help of Dr. Bryon Grove and Ms. Sarah Abrahamson in using the Edward C. Carlson Imaging and Image Analysis Core Facility. This work was supported by grants from the National Institutes of Health including P30GM103329, R01MH100972, R01MH105329, and R21DA040519.

## References

- [1]. Blennow K, de Leon MJ, Zetterberg H (2006) Alzheimer's disease. *Lancet* 368, 387–403. [PubMed: 16876668]
- [2]. Hardy J (2009) The amyloid hypothesis for Alzheimer's disease: a critical reappraisal. *J Neurochem* 110, 1129–1134. [PubMed: 19457065]
- [3]. Seabrook GR, Ray WJ, Shearman M, Hutton M (2007) Beyond amyloid: the next generation of Alzheimer's disease therapeutics. *Mol Interv* 7, 261–270. [PubMed: 17932415]
- [4]. Nixon RA, Cataldo AM, Mathews PM (2000) The endosomal-lysosomal system of neurons in Alzheimer's disease pathogenesis: a review. *Neurochem Res* 25, 1161–1172. [PubMed: 11059790]
- [5]. Goate A, Hardy J (2012) Twenty years of Alzheimer's disease-causing mutations. *J Neurochem* 120 Suppl 1, 3–8. [PubMed: 22122678]
- [6]. Holtzman DM, Morris JC, Goate AM (2011) Alzheimer's disease: the challenge of the second century. *Sci Transl Med* 3, 77sr71.

- [7]. Reitz C, Brayne C, Mayeux R (2011) Epidemiology of Alzheimer disease. *Nat Rev Neurol* 7, 137–152. [PubMed: 21304480]
- [8]. Solomon A, Kivipelto M, Wolozin B, Zhou J, Whitmer RA (2009) Midlife serum cholesterol and increased risk of Alzheimer's and vascular dementia three decades later. *Dement Geriatr Cogn Disord* 28, 75–80. [PubMed: 19648749]
- [9]. Chen X, Wagener JF, Morgan DH, Hui L, Ghribi O, Geiger JD (2010) Endolysosome Mechanisms Associated with Alzheimer's Disease-like Pathology in Rabbits Ingesting Cholesterol-Enriched Diet. *J Alzheimers Dis* 22, 1289–1303. [PubMed: 20930277]
- [10]. Hui L, Chen X, Geiger JD (2012) Endolysosome involvement in LDL cholesterol-induced Alzheimer's disease-like pathology in primary cultured neurons. *Life Sci* 91, 1159–1168. [PubMed: 22580286]
- [11]. Reed B, Villeneuve S, Mack W, DeCarli C, Chui HC, Jagust W (2014) Associations between serum cholesterol levels and cerebral amyloidosis. *JAMA Neurol* 71, 195–200. [PubMed: 24378418]
- [12]. Lesser GT, Beeri MS, Schmeidler J, Purohit DP, Haroutunian V (2011) Cholesterol and LDL relate to neuritic plaques and to APOE4 presence but not to neurofibrillary tangles. *Curr Alzheimer Res* 8, 303–312. [PubMed: 21244352]
- [13]. Farrer LA, Cupples LA, Haines JL, Hyman B, Kukull WA, Mayeux R, Myers RH, Pericak-Vance MA, Risch N, van Duijn CM (1997) Effects of age, sex, and ethnicity on the association between apolipoprotein E genotype and Alzheimer disease. A meta-analysis. APOE and Alzheimer Disease Meta Analysis Consortium. *JAMA* 278, 1349–1356. [PubMed: 9343467]
- [14]. Corder EH, Saunders AM, Strittmatter WJ, Schmechel DE, Gaskell PC, Small GW, Roses AD, Haines JL, Pericak-Vance MA (1993) Gene dose of apolipoprotein E type 4 allele and the risk of Alzheimer's disease in late onset families. *Science* 261, 921–923. [PubMed: 8346443]
- [15]. Marzolo MP, Bu G (2009) Lipoprotein receptors and cholesterol in APP trafficking and proteolytic processing, implications for Alzheimer's disease. *Semin Cell Dev Biol* 20, 191–200. [PubMed: 19041409]
- [16]. Strand BH, Langballe EM, Hjellvik V, Handal M, Naess O, Knudsen GP, Refsum H, Tambs K, Nafstad P, Schirmer H, Bergem AL, Selmer R, Engedal K, Magnus P, Bjertness E (2013) Midlife vascular risk factors and their association with dementia deaths: results from a Norwegian prospective study followed up for 35 years. *J Neurol Sci* 324, 124–130. [PubMed: 23146611]
- [17]. Notkola IL, Sulkava R, Pekkanen J, Erkinjuntti T, Ehnholm C, Kivinen P, Tuomilehto J, Nissinen A (1998) Serum total cholesterol, apolipoprotein E epsilon 4 allele, and Alzheimer's disease. *Neuroepidemiology* 17, 14–20. [PubMed: 9549720]
- [18]. Kivipelto M, Helkala EL, Laakso MP, Hanninen T, Hallikainen M, Alhainen K, Iivonen S, Mannermaa A, Tuomilehto J, Nissinen A, Soininen H (2002) Apolipoprotein E epsilon4 allele, elevated midlife total cholesterol level, and high midlife systolic blood pressure are independent risk factors for late-life Alzheimer disease. *Ann Intern Med* 137, 149–155. [PubMed: 12160362]
- [19]. Kuo YM, Emmerling MR, Bisgaier CL, Essenburg AD, Lampert HC, Drumm D, Roher AE (1998) Elevated low-density lipoprotein in Alzheimer's disease correlates with brain abeta 1–42 levels. *Biochem Biophys Res Commun* 252, 711–715. [PubMed: 9837771]
- [20]. Matsuzaki T, Sasaki K, Hata J, Hirakawa Y, Fujimi K, Ninomiya T, Suzuki SO, Kanba S, Kiyohara Y, Iwaki T (2011) Association of Alzheimer disease pathology with abnormal lipid metabolism: the Hisayama Study. *Neurology* 77, 1068–1075. [PubMed: 21911734]
- [21]. Reitz C, Tang MX, Schupf N, Manly JJ, Mayeux R, Luchsinger JA (2010) Association of higher levels of high-density lipoprotein cholesterol in elderly individuals and lower risk of late-onset Alzheimer disease. *Arch Neurol* 67, 1491–1497. [PubMed: 21149810]
- [22]. Yasuno F, Asada T (2013) Effect of plasma lipids and APOE genotype on cognitive decline. *Dialogues Clin Neurosci* 15, 120–126. [PubMed: 23576895]
- [23]. Bjorkhem I, Meaney S (2004) Brain cholesterol: long secret life behind a barrier. *Arterioscler Thromb Vasc Biol* 24, 806–815. [PubMed: 14764421]
- [24]. Pitas RE, Boyles JK, Lee SH, Hui D, Weisgraber KH (1987) Lipoproteins and their receptors in the central nervous system. Characterization of the lipoproteins in cerebrospinal fluid and

- identification of apolipoprotein B,E(LDL) receptors in the brain. *J Biol Chem* 262, 14352–14360. [PubMed: 3115992]
- [25]. Zipser BD, Johanson CE, Gonzalez L, Berzin TM, Tavares R, Hulette CM, Vitek MP, Hovanesian V, Stopa EG (2007) Microvascular injury and blood-brain barrier leakage in Alzheimer's disease. *Neurobiol Aging* 28, 977–986. [PubMed: 16782234]
- [26]. Ujiie M, Dickstein DL, Carlow DA, Jefferies WA (2003) Blood-brain barrier permeability precedes senile plaque formation in an Alzheimer disease model. *Microcirculation* 10, 463–470. [PubMed: 14745459]
- [27]. Kalaria RN (1999) The blood-brain barrier and cerebrovascular pathology in Alzheimer's disease. *Ann N Y Acad Sci* 893, 113–125. [PubMed: 10672233]
- [28]. Kalaria RN (1992) The blood-brain barrier and cerebral microcirculation in Alzheimer disease. *Cerebrovasc Brain Metab Rev* 4, 226–260. [PubMed: 1389957]
- [29]. Munoz DG, Erkinjuntti T, Gaytan-Garcia S, Hachinski V (1997) Serum protein leakage in Alzheimer's disease revisited. *Ann N Y Acad Sci* 826, 173–189. [PubMed: 9329689]
- [30]. Bell RD, Winkler EA, Singh I, Sagare AP, Deane R, Wu Z, Holtzman DM, Betsholtz C, Armulik A, Sallstrom J, Berk BC, Zlokovic BV (2012) Apolipoprotein E controls cerebrovascular integrity via cyclophilin A. *Nature* 485, 512–516. [PubMed: 22622580]
- [31]. Saeed AA, Genove G, Li T, Lutjohann D, Olin M, Mast N, Pikuleva IA, Crick P, Wang Y, Griffiths W, Betsholtz C, Bjorkhem I (2014) Effects of a disrupted blood-brain barrier on cholesterol homeostasis in the brain. *J Biol Chem* 289, 23712–23722. [PubMed: 24973215]
- [32]. Namba Y, Tsuchiya H, Ikeda K (1992) Apolipoprotein B immunoreactivity in senile plaque and vascular amyloids and neurofibrillary tangles in the brains of patients with Alzheimer's disease. *Neurosci Lett* 134, 264–266. [PubMed: 1375354]
- [33]. Takechi R, Galloway S, Pallegage-Gamarallage M, Wellington C, Johnsen R, Mamo JC (2009) Three-dimensional colocalization analysis of plasma-derived apolipoprotein B with amyloid plaques in APP/PS1 transgenic mice. *Histochem Cell Biol* 131, 661–666. [PubMed: 19225804]
- [34]. Berezcki E, Bernat G, Csont T, Ferdinandy P, Scheich H, Santha M (2008) Overexpression of human apolipoprotein B-100 induces severe neurodegeneration in transgenic mice. *J Proteome Res* 7, 2246–2252. [PubMed: 18473452]
- [35]. Kanoski SE, Zhang Y, Zheng W, Davidson TL (2010) The effects of a high-energy diet on hippocampal function and blood-brain barrier integrity in the rat. *J Alzheimers Dis* 21, 207–219. [PubMed: 20413889]
- [36]. Davidson TL, Monnot A, Neal AU, Martin AA, Horton JJ, Zheng W (2012) The effects of a high-energy diet on hippocampal-dependent discrimination performance and blood-brain barrier integrity differ for diet-induced obese and diet-resistant rats. *Physiol Behav* 107, 26–33. [PubMed: 22634281]
- [37]. Freeman LR, Granholm AC (2012) Vascular changes in rat hippocampus following a high saturated fat and cholesterol diet. *J Cereb Blood Flow Metab* 32, 643–653. [PubMed: 22108721]
- [38]. Chen X, Gawryluk JW, Wagener JF, Ghribi O, Geiger JD (2008) Caffeine blocks disruption of blood brain barrier in a rabbit model of Alzheimer's disease. *J Neuroinflammation* 5, 12. [PubMed: 18387175]
- [39]. Cataldo AM, Barnett JL, Pieroni C, Nixon RA (1997) Increased neuronal endocytosis and protease delivery to early endosomes in sporadic Alzheimer's disease: neuropathologic evidence for a mechanism of increased beta-amyloidogenesis. *J Neurosci* 17, 6142–6151. [PubMed: 9236226]
- [40]. Nixon RA, Cataldo AM (2006) Lysosomal system pathways: genes to neurodegeneration in Alzheimer's disease. *Journal of Alzheimer's disease : JAD* 9, 277–289. [PubMed: 16914867]
- [41]. Wolfe DM, Lee JH, Kumar A, Lee S, Orenstein SJ, Nixon RA (2013) Autophagy failure in Alzheimer's disease and the role of defective lysosomal acidification. *Eur J Neurosci* 37, 1949–1961. [PubMed: 23773064]
- [42]. Greeve J, Altkemper I, Dieterich JH, Greten H, Windler E (1993) Apolipoprotein B mRNA editing in 12 different mammalian species: hepatic expression is reflected in low concentrations of apoB-containing plasma lipoproteins. *J Lipid Res* 34, 1367–1383. [PubMed: 8409768]



- [43]. Innerarity TL, Pitas RE, Mahley RW (1980) Disparities in the interaction of rat and human lipoproteins with cultured rat fibroblasts and smooth muscle cells. Requirements for homology for receptor binding activity. *J Biol Chem* 255, 11163–11172. [PubMed: 6254962]
- [44]. de Chaves EP, Narayanaswami V (2008) Apolipoprotein E and cholesterol in aging and disease in the brain. *Future Lipidol* 3, 505–530. [PubMed: 19649144]
- [45]. Vance JE (2012) Dysregulation of cholesterol balance in the brain: contribution to neurodegenerative diseases. *Dis Model Mech* 5, 746–755. [PubMed: 23065638]
- [46]. Ulrich JD, Burchett JM, Restivo JL, Schuler DR, Verghese PB, Mahan TE, Landreth GE, Castellano JM, Jiang H, Cirrito JR, Holtzman DM (2013) In vivo measurement of apolipoprotein E from the brain interstitial fluid using microdialysis. *Mol Neurodegener* 8, 13. [PubMed: 23601557]
- [47]. Chantepie S, Bochem AE, Chapman MJ, Hovingh GK, Kontush A (2012) High-density lipoprotein (HDL) particle subpopulations in heterozygous cholesteryl ester transfer protein (CETP) deficiency: maintenance of antioxidative activity. *PLoS One* 7, e49336. [PubMed: 23189141]
- [48]. Miida T, Yamazaki F, Sakurai M, Wada R, Yamadera T, Asami K, Hoshiyama M, Tanaka A, Inano K, Okada M (1999) The apolipoprotein E content of HDL in cerebrospinal fluid is higher in children than in adults. *Clin Chem* 45, 1294–1296. [PubMed: 10430802]
- [49]. Rajendran L, Annaert W (2012) Membrane trafficking pathways in Alzheimer's disease. *Traffic* 13, 759–770. [PubMed: 22269004]
- [50]. Morel E, Chamoun Z, Lasiecka ZM, Chan RB, Williamson RL, Vetanovetz C, Dall'Armi C, Simoes S, Point Du Jour KS, McCabe BD, Small SA, Di Paolo G (2013) Phosphatidylinositol-3-phosphate regulates sorting and processing of amyloid precursor protein through the endosomal system. *Nat Commun* 4, 2250. [PubMed: 23907271]
- [51]. Shen D, Wang X, Li X, Zhang X, Yao Z, Dibble S, Dong XP, Yu T, Lieberman AP, Showalter HD, Xu H (2012) Lipid storage disorders block lysosomal trafficking by inhibiting a TRP channel and lysosomal calcium release. *Nat Commun* 3, 731. [PubMed: 22415822]
- [52]. Youmans KL, Tai LM, Kanekiyo T, Stine WB, Jr., Michon SC, Nwabuisi-Heath E, Manelli AM, Fu Y, Riordan S, Eimer WA, Binder L, Bu G, Yu C, Hartley DM, LaDu MJ (2012) Intraneuronal Aβ detection in 5xFAD mice by a new Aβ-specific antibody. *Mol Neurodegener* 7, 8. [PubMed: 22423893]
- [53]. Nieweg K, Schaller H, Pfrieger FW (2009) Marked differences in cholesterol synthesis between neurons and glial cells from postnatal rats. *J Neurochem* 109, 125–134. [PubMed: 19166509]
- [54]. Oller-Salvia B, Sanchez-Navarro M, Giralte E, Teixido M (2016) Blood-brain barrier shuttle peptides: an emerging paradigm for brain delivery. *Chem Soc Rev* 45, 4690–4707. [PubMed: 27188322]
- [55]. Koch S, Donarski N, Goetze K, Kreckel M, Stuerenburg HJ, Buhmann C, Beisiegel U (2001) Characterization of four lipoprotein classes in human cerebrospinal fluid. *J Lipid Res* 42, 1143–1151. [PubMed: 11441143]
- [56]. Wang H, Eckel RH (2014) What are lipoproteins doing in the brain? *Trends Endocrinol Metab* 25, 8–14. [PubMed: 24189266]
- [57]. Chakraborty A, de Wit NM, van der Flier WM, de Vries HE (2017) The blood brain barrier in Alzheimer's disease. *Vascul Pharmacol* 89, 12–18. [PubMed: 27894893]
- [58]. Barnes DE, Yaffe K (2011) The projected effect of risk factor reduction on Alzheimer's disease prevalence. *Lancet Neurol* 10, 819–828. [PubMed: 21775213]
- [59]. Hasnain M, Vieweg WV (2014) Possible role of vascular risk factors in Alzheimer's disease and vascular dementia. *Curr Pharm Des* 20, 6007–6013. [PubMed: 24641219]
- [60]. Ference BA, Ginsberg HN, Graham I, Ray KK, Packard CJ, Bruckert E, Hegele RA, Krauss RM, Raal FJ, Schunkert H, Watts GF, Boren J, Fazio S, Horton JD, Masana L, Nicholls SJ, Nordestgaard BG, van de Sluis B, Taskiran MR, Tokgozoglu L, Landmesser U, Laufs U, Wiklund O, Stock JK, Chapman MJ, Catapano AL (2017) Low-density lipoproteins cause atherosclerotic cardiovascular disease. 1. Evidence from genetic, epidemiologic, and clinical studies. A consensus statement from the European Atherosclerosis Society Consensus Panel. *Eur Heart J* 38, 2459–2472. [PubMed: 28444290]



- [61]. Schreurs MP, Hubel CA, Bernstein IM, Jeyabalan A, Cipolla MJ (2013) Increased oxidized low-density lipoprotein causes blood-brain barrier disruption in early-onset preeclampsia through LOX-1. *FASEB J* 27, 1254–1263. [PubMed: 23230281]
- [62]. Acharya NK, Levin EC, Clifford PM, Han M, Tourtellotte R, Chamberlain D, Pollaro M, Coretti NJ, Kosciuk MC, Nagele EP, Demarshall C, Freeman T, Shi Y, Guan C, Macphee CH, Wilensky RL, Nagele RG (2013) Diabetes and hypercholesterolemia increase blood-brain barrier permeability and brain amyloid deposition: beneficial effects of the LpPLA2 inhibitor darapladib. *J Alzheimers Dis* 35, 179–198. [PubMed: 23388174]
- [63]. Montagne A, Barnes SR, Sweeney MD, Halliday MR, Sagare AP, Zhao Z, Toga AW, Jacobs RE, Liu CY, Amezcua L, Harrington MG, Chui HC, Law M, Zlokovic BV (2015) Blood-brain barrier breakdown in the aging human hippocampus. *Neuron* 85, 296–302. [PubMed: 25611508]
- [64]. van de Haar HJ, Burgmans S, Jansen JF, van Osch MJ, van Buchem MA, Muller M, Hofman PA, Verhey FR, Backes WH (2016) Blood-Brain Barrier Leakage in Patients with Early Alzheimer Disease. *Radiology* 281, 527–535. [PubMed: 27243267]
- [65]. van de Haar HJ, Jansen JFA, Jeukens C, Burgmans S, van Buchem MA, Muller M, Hofman PAM, Verhey FRJ, van Osch MJP, Backes WH (2017) Subtle blood-brain barrier leakage rate and spatial extent: Considerations for dynamic contrast-enhanced MRI. *Med Phys* 44, 4112–4125. [PubMed: 28493613]
- [66]. van de Haar HJ, Jansen JFA, van Osch MJP, van Buchem MA, Muller M, Wong SM, Hofman PAM, Burgmans S, Verhey FRJ, Backes WH (2016) Neurovascular unit impairment in early Alzheimer's disease measured with magnetic resonance imaging. *Neurobiol Aging* 45, 190–196. [PubMed: 27459939]
- [67]. Shams S, Granberg T, Martola J, Charidimou A, Li X, Shams M, Fereshtehnejad SM, Cavallin L, Aspelin P, Wiberg-Kristoffersen M, Wahlund LO (2017) Cerebral microbleeds topography and cerebrospinal fluid biomarkers in cognitive impairment. *J Cereb Blood Flow Metab* 37, 1006–1013. [PubMed: 27178426]
- [68]. Shams S, Wahlund LO (2016) Cerebral microbleeds as a biomarker in Alzheimer's disease? A review in the field. *Biomark Med* 10, 9–18. [PubMed: 26641942]
- [69]. Brundel M, Heringa SM, de Bresser J, Koek HL, Zwanenburg JJ, Jaap Kappelle L, Luijten PR, Biessels GJ (2012) High prevalence of cerebral microbleeds at 7Tesla MRI in patients with early Alzheimer's disease. *J Alzheimers Dis* 31, 259–263. [PubMed: 22531417]
- [70]. Tsai HH, Tsai LK, Chen YF, Tang SC, Lee BC, Yen RF, Jeng JS (2017) Correlation of Cerebral Microbleed Distribution to Amyloid Burden in Patients with Primary Intracerebral Hemorrhage. *Sci Rep* 7, 44715. [PubMed: 28303922]
- [71]. Nelson AR, Sweeney MD, Sagare AP, Zlokovic BV (2016) Neurovascular dysfunction and neurodegeneration in dementia and Alzheimer's disease. *Biochim Biophys Acta* 1862, 887–900. [PubMed: 26705676]
- [72]. Takechi R, Galloway S, Pallegage-Gamarallage MM, Wellington CL, Johnsen RD, Dhaliwal SS, Mamo JC (2010) Differential effects of dietary fatty acids on the cerebral distribution of plasma-derived apo B lipoproteins with amyloid-beta. *Br J Nutr* 103, 652–662. [PubMed: 19860996]
- [73]. Niwa A, Ii Y, Shindo A, Matsuo K, Ishikawa H, Taniguchi A, Takase S, Maeda M, Sakuma H, Akatsu H, Hashizume Y, Tomimoto H (2017) Comparative Analysis of Cortical Microinfarcts and Microbleeds using 3.0-Tesla Postmortem Magnetic Resonance Images and Histopathology. *J Alzheimers Dis* 59, 951–959. [PubMed: 28697558]
- [74]. Laatsch A, Panteli M, Sornsakrin M, Hoffzimmer B, Grewal T, Heeren J (2012) Low density lipoprotein receptor-related protein 1 dependent endosomal trapping and recycling of apolipoprotein E. *PLoS One* 7, e29385. [PubMed: 22238606]
- [75]. Rensen PC, Jong MC, van Vark LC, van der Boom H, Hendriks WL, van Berkel TJ, Biessen EA, Havekes LM (2000) Apolipoprotein E is resistant to intracellular degradation in vitro and in vivo. Evidence for retroendocytosis. *J Biol Chem* 275, 8564–8571. [PubMed: 10722695]
- [76]. Heeren J, Grewal T, Laatsch A, Rottke D, Rinninger F, Enrich C, Beisiegel U (2003) Recycling of apoprotein E is associated with cholesterol efflux and high density lipoprotein internalization. *J Biol Chem* 278, 14370–14378. [PubMed: 12584196]

- [77]. Heeren J, Grewal T, Laatsch A, Becker N, Rinninger F, Rye KA, Beisiegel U (2004) Impaired recycling of apolipoprotein E4 is associated with intracellular cholesterol accumulation. *J Biol Chem* 279, 55483–55492. [PubMed: 15485881]
- [78]. Chen Y, Durakoglugil MS, Xian X, Herz J (2010) ApoE4 reduces glutamate receptor function and synaptic plasticity by selectively impairing ApoE receptor recycling. *Proc Natl Acad Sci U S A* 107, 12011–12016. [PubMed: 20547867]
- [79]. Chen X, Wagener JF, Morgan DH, Hui L, Ghribi O, Geiger JD (2010) Endolysosome mechanisms associated with Alzheimer's disease-like pathology in rabbits ingesting cholesterol-enriched diet. *Journal of Alzheimer's disease : JAD* 22, 1289–1303. [PubMed: 20930277]
- [80]. Cataldo AM, Peterhoff CM, Troncoso JC, Gomez-Isla T, Hyman BT, Nixon RA (2000) Endocytic pathway abnormalities precede amyloid beta deposition in sporadic Alzheimer's disease and Down syndrome: differential effects of APOE genotype and presenilin mutations. *Am J Pathol* 157, 277–286. [PubMed: 10880397]
- [81]. Cataldo AM, Hamilton DJ, Nixon RA (1994) Lysosomal abnormalities in degenerating neurons link neuronal compromise to senile plaque development in Alzheimer disease. *Brain Res* 640, 68–80. [PubMed: 8004466]
- [82]. Nixon RA (2005) Endosome function and dysfunction in Alzheimer's disease and other neurodegenerative diseases. *Neurobiol Aging* 26, 373–382. [PubMed: 15639316]
- [83]. Coffey EE, Beckel JM, Laties AM, Mitchell CH (2014) Lysosomal alkalization and dysfunction in human fibroblasts with the Alzheimer's disease-linked presenilin 1 A246E mutation can be reversed with cAMP. *Neuroscience* 263, 111–124. [PubMed: 24418614]
- [84]. Lee JH, Yu WH, Kumar A, Lee S, Mohan PS, Peterhoff CM, Wolfe DM, Martinez-Vicente M, Massey AC, Sovak G, Uchiyama Y, Westaway D, Cuervo AM, Nixon RA (2010) Lysosomal proteolysis and autophagy require presenilin 1 and are disrupted by Alzheimer-related PS1 mutations. *Cell* 141, 1146–1158. [PubMed: 20541250]
- [85]. Yang DS, Stavrides P, Saito M, Kumar A, Rodriguez-Navarro JA, Pawlik M, Huo C, Walkley SU, Saito M, Cuervo AM, Nixon RA (2014) Defective macroautophagic turnover of brain lipids in the TgCRND8 Alzheimer mouse model: prevention by correcting lysosomal proteolytic deficits. *Brain* 137, 3300–3318. [PubMed: 25270989]
- [86]. Torres M, Jimenez S, Sanchez-Varo R, Navarro V, Trujillo-Estrada L, Sanchez-Mejias E, Carmona I, Davila JC, Vizuete M, Gutierrez A, Vitorica J (2012) Defective lysosomal proteolysis and axonal transport are early pathogenic events that worsen with age leading to increased APP metabolism and synaptic Abeta in transgenic APP/PS1 hippocampus. *Mol Neurodegener* 7, 59. [PubMed: 23173743]
- [87]. Bergmann M, Schutt F, Holz FG, Kopitz J (2004) Inhibition of the ATP-driven proton pump in RPE lysosomes by the major lipofuscin fluorophore A2-E may contribute to the pathogenesis of age-related macular degeneration. *FASEB J* 18, 562–564. [PubMed: 14715704]
- [88]. Porter K, Nallathambi J, Lin Y, Liton PB (2013) Lysosomal basification and decreased autophagic flux in oxidatively stressed trabecular meshwork cells: implications for glaucoma pathogenesis. *Autophagy* 9, 581–594. [PubMed: 23360789]
- [89]. Butterfield DA, Di Domenico F, Swomley AM, Head E, Perluigi M (2014) Redox proteomics analysis to decipher the neurobiology of Alzheimer-like neurodegeneration: overlaps in Down's syndrome and Alzheimer's disease brain. *Biochem J* 463, 177–189. [PubMed: 25242166]
- [90]. Cox BE, Griffin EE, Ullery JC, Jerome WG (2007) Effects of cellular cholesterol loading on macrophage foam cell lysosome acidification. *J Lipid Res* 48, 1012–1021. [PubMed: 17308299]
- [91]. Finnigan GC, Ryan M, Stevens TH (2011) A genome-wide enhancer screen implicates sphingolipid composition in vacuolar ATPase function in *Saccharomyces cerevisiae*. *Genetics* 187, 771–783. [PubMed: 21196517]
- [92]. Myers BM, Prendergast FG, Holman R, Kuntz SM, LaRusso NF (1991) Alterations in the structure, physicochemical properties, and pH of hepatocyte lysosomes in experimental iron overload. *J Clin Invest* 88, 1207–1215. [PubMed: 1918375]
- [93]. Kao JK, Wang SC, Ho LW, Huang SW, Chang SH, Yang RC, Ke YY, Wu CY, Wang JY, Shieh JJ (2016) Chronic Iron Overload Results in Impaired Bacterial Killing of THP-1 Derived

Macrophage through the Inhibition of Lysosomal Acidification. *PLoS One* 11, e0156713. [PubMed: 27244448]

- [94]. Fernandez B, Fdez E, Gomez-Suaga P, Gil F, Molina-Villalba I, Ferrer I, Patel S, Churchill GC, Hilfiker S (2016) Iron overload causes endolysosomal deficits modulated by NAADP-regulated 2-pore channels and RAB7A. *Autophagy* 12, 1487–1506. [PubMed: 27383256]
- [95]. Hui L, Chen X, Geiger JD (2012) Endolysosome involvement in LDL cholesterol-induced Alzheimer's disease-like pathology in primary cultured neurons. *Life sciences* 91, 1159–1168. [PubMed: 22580286]
- [96]. Nixon RA (2007) Autophagy, amyloidogenesis and Alzheimer disease. *Journal of cell science* 120, 4081–4091. [PubMed: 18032783]
- [97]. Hamazaki H (1996) Cathepsin D is involved in the clearance of Alzheimer's beta-amyloid protein. *FEBS Lett* 396, 139–142. [PubMed: 8914975]
- [98]. Ladror US, Snyder SW, Wang GT, Holzman TF, Krafft GA (1994) Cleavage at the amino and carboxyl termini of Alzheimer's amyloid-beta by cathepsin D. *J Biol Chem* 269, 18422–18428. [PubMed: 8034590]
- [99]. Saftig P, Peters C, von Figura K, Craessaerts K, Van Leuven F, De Strooper B (1996) Amyloidogenic processing of human amyloid precursor protein in hippocampal neurons devoid of cathepsin D. *J Biol Chem* 271, 27241–27244. [PubMed: 8910296]
- [100]. Di Domenico F, Tramutola A, Perluigi M (2016) Cathepsin D as a therapeutic target in Alzheimer's disease. *Expert Opin Ther Targets* 20, 1393–1395. [PubMed: 27805462]
- [101]. Yuyama K, Yamamoto N, Yanagisawa K (2006) Chloroquine-induced endocytic pathway abnormalities: Cellular model of GM1 ganglioside-induced Abeta fibrillogenesis in Alzheimer's disease. *FEBS Lett* 580, 6972–6976. [PubMed: 17161396]
- [102]. Chen PM, Gombart ZJ, Chen JW (2011) Chloroquine treatment of ARPE-19 cells leads to lysosome dilation and intracellular lipid accumulation: possible implications of lysosomal dysfunction in macular degeneration. *Cell Biosci* 1, 10. [PubMed: 21711726]
- [103]. Vingtdoux V, Hamdane M, Loyens A, Gele P, Drobeck H, Begard S, Galas MC, Delacourte A, Beauvillain JC, Buee L, Sergeant N (2007) Alkalinizing drugs induce accumulation of amyloid precursor protein by-products in luminal vesicles of multivesicular bodies. *J Biol Chem* 282, 18197–18205. [PubMed: 17468104]
- [104]. Schrader-Fischer G, Paganetti PA (1996) Effect of alkalizing agents on the processing of the beta-amyloid precursor protein. *Brain Res* 716, 91–100. [PubMed: 8738224]
- [105]. Mielke JG, Murphy MP, Maritz J, Bengualid KM, Ivy GO (1997) Chloroquine administration in mice increases beta-amyloid immunoreactivity and attenuates kainate-induced blood-brain barrier dysfunction. *Neurosci Lett* 227, 169–172. [PubMed: 9185677]
- [106]. Knops J, Suomensaaari S, Lee M, McConlogue L, Seubert P, Sinha S (1995) Cell-type and amyloid precursor protein-type specific inhibition of A beta release by bafilomycin A1, a selective inhibitor of vacuolar ATPases. *J Biol Chem* 270, 2419–2422. [PubMed: 7852298]
- [107]. Haass C, Capell A, Citron M, Teplow DB, Selkoe DJ (1995) The vacuolar H(+)-ATPase inhibitor bafilomycin A1 differentially affects proteolytic processing of mutant and wild-type beta-amyloid precursor protein. *J Biol Chem* 270, 6186–6192. [PubMed: 7890753]
- [108]. Lafourcade C, Sobo K, Kieffer-Jaquinod S, Garin J, van der Goot FG (2008) Regulation of the V-ATPase along the endocytic pathway occurs through reversible subunit association and membrane localization. *PLoS One* 3, e2758. [PubMed: 18648502]
- [109]. Chung J, Phukan G, Vergote D, Mohamed A, Maulik M, Stahn M, Andrew RJ, Thinakaran G, Posse de Chaves E, Kar S (2018) Endosomal-Lysosomal Cholesterol Sequestration by U18666A Differentially Regulates Amyloid Precursor Protein (APP) Metabolism in Normal and APP-Overexpressing Cells. *Mol Cell Biol* 38.
- [110]. Avrahami L, Farfara D, Shaham-Kol M, Vassar R, Frenkel D, Eldar-Finkelman H (2013) Inhibition of glycogen synthase kinase-3 ameliorates beta-amyloid pathology and restores lysosomal acidification and mammalian target of rapamycin activity in the Alzheimer disease mouse model: in vivo and in vitro studies. *J Biol Chem* 288, 1295–1306. [PubMed: 23155049]

- [111]. Bourdenx M, Daniel J, Genin E, Soria FN, Blanchard-Desce M, Bezard E, Dehay B (2016) Nanoparticles restore lysosomal acidification defects: Implications for Parkinson and other lysosomal-related diseases. *Autophagy* 12, 472–483. [PubMed: 26761717]
- [112]. Baltazar GC, Guha S, Lu W, Lim J, Boesze-Battaglia K, Laties AM, Tyagi P, Kompella UB, Mitchell CH (2012) Acidic nanoparticles are trafficked to lysosomes and restore an acidic lysosomal pH and degradative function to compromised ARPE-19 cells. *PLoS One* 7, e49635. [PubMed: 23272048]
- [113]. Sanchez-Lopez E, Ettcheto M, Egea MA, Espina M, Cano A, Calpena AC, Camins A, Carmona N, Silva AM, Souto EB, Garcia ML (2018) Memantine loaded PLGA PEGylated nanoparticles for Alzheimer's disease: in vitro and in vivo characterization. *J Nanobiotechnology* 16, 32. [PubMed: 29587747]
- [114]. Shimizu H, Tosaki A, Kaneko K, Hisano T, Sakurai T, Nukina N (2008) Crystal structure of an active form of BACE1, an enzyme responsible for amyloid beta protein production. *Mol Cell Biol* 28, 3663–3671. [PubMed: 18378702]
- [115]. Rajendran L, Schneider A, Schlechtingen G, Weidlich S, Ries J, Braxmeier T, Schwille P, Schulz JB, Schroeder C, Simons M, Jennings G, Knolker HJ, Simons K (2008) Efficient inhibition of the Alzheimer's disease beta-secretase by membrane targeting. *Science* 320, 520–523. [PubMed: 18436784]
- [116]. Koh YH, von Arnim CA, Hyman BT, Tanzi RE, Tesco G (2005) BACE is degraded via the lysosomal pathway. *J Biol Chem* 280, 32499–32504. [PubMed: 16033761]
- [117]. Barrett AJ (1970) Cathepsin D. Purification of isoenzymes from human and chicken liver. *Biochem J* 117, 601–607. [PubMed: 5419752]
- [118]. Tam JH, Seah C, Pasternak SH (2014) The Amyloid Precursor Protein is rapidly transported from the Golgi apparatus to the lysosome and where it is processed into beta-amyloid. *Mol Brain* 7, 54. [PubMed: 25085554]
- [119]. Zhong XZ, Sun X, Cao Q, Dong G, Schiffmann R, Dong XP (2016) BK channel agonist represents a potential therapeutic approach for lysosomal storage diseases. *Sci Rep* 6, 33684. [PubMed: 27670435]
- [120]. Cao Q, Zhong XZ, Zou Y, Zhang Z, Toro L, Dong XP (2015) BK Channels Alleviate Lysosomal Storage Diseases by Providing Positive Feedback Regulation of Lysosomal Ca<sup>2+</sup> Release. *Dev Cell* 33, 427–441. [PubMed: 25982675]
- [121]. Ishida Y, Nayak S, Mindell JA, Grabe M (2013) A model of lysosomal pH regulation. *J Gen Physiol* 141, 705–720. [PubMed: 23712550]
- [122]. Li SC, Diakov TT, Xu T, Tarsio M, Zhu W, Couoh-Cardel S, Weisman LS, Kane PM (2014) The signaling lipid PI(3,5)P(2) stabilizes V(1)-V(o) sector interactions and activates the V-ATPase. *Mol Biol Cell* 25, 1251–1262. [PubMed: 24523285]

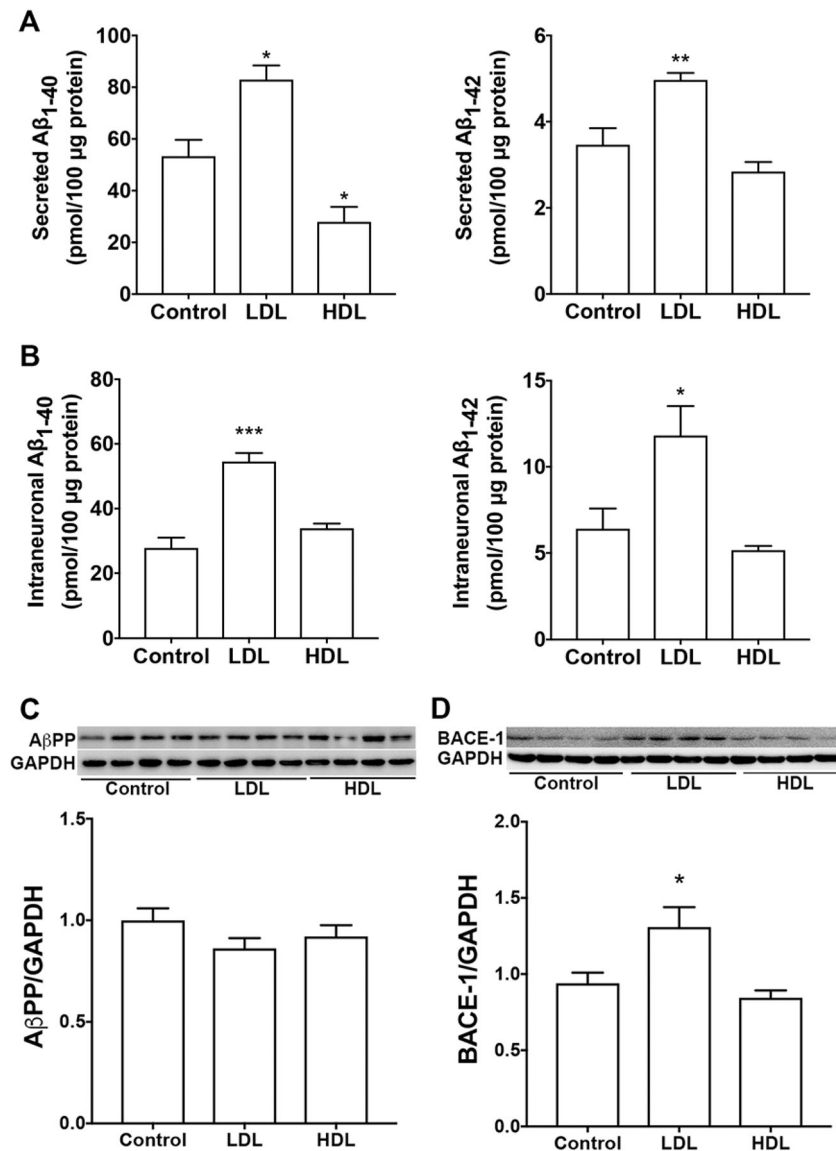


**Figure 1. LDL, but not HDL, increased Aβ.**

(A, B) In SH-SY5Y cells expressing wild-type AβPP, LDL (50 μg/ml for 3 days) treatment significantly increased secreted levels Aβ<sub>1-40</sub> and Aβ<sub>1-42</sub>, as well as, intraneuronal levels of Aβ<sub>1-40</sub> and Aβ<sub>1-42</sub> (\*p<0.05; \*\*p<0.01; \*\*\*p<0.001 vs control; n=5). HDL (50 μg/ml for 3 days) treatment did not significantly increase secreted or intraneuronal levels of Aβ (n=5). (C) Neither LDL nor HDL affected protein levels of full-length AβPP. (D) LDL treatment, but not HDL, increased significantly protein levels of BACE1 (\*p<0.05; n=4).

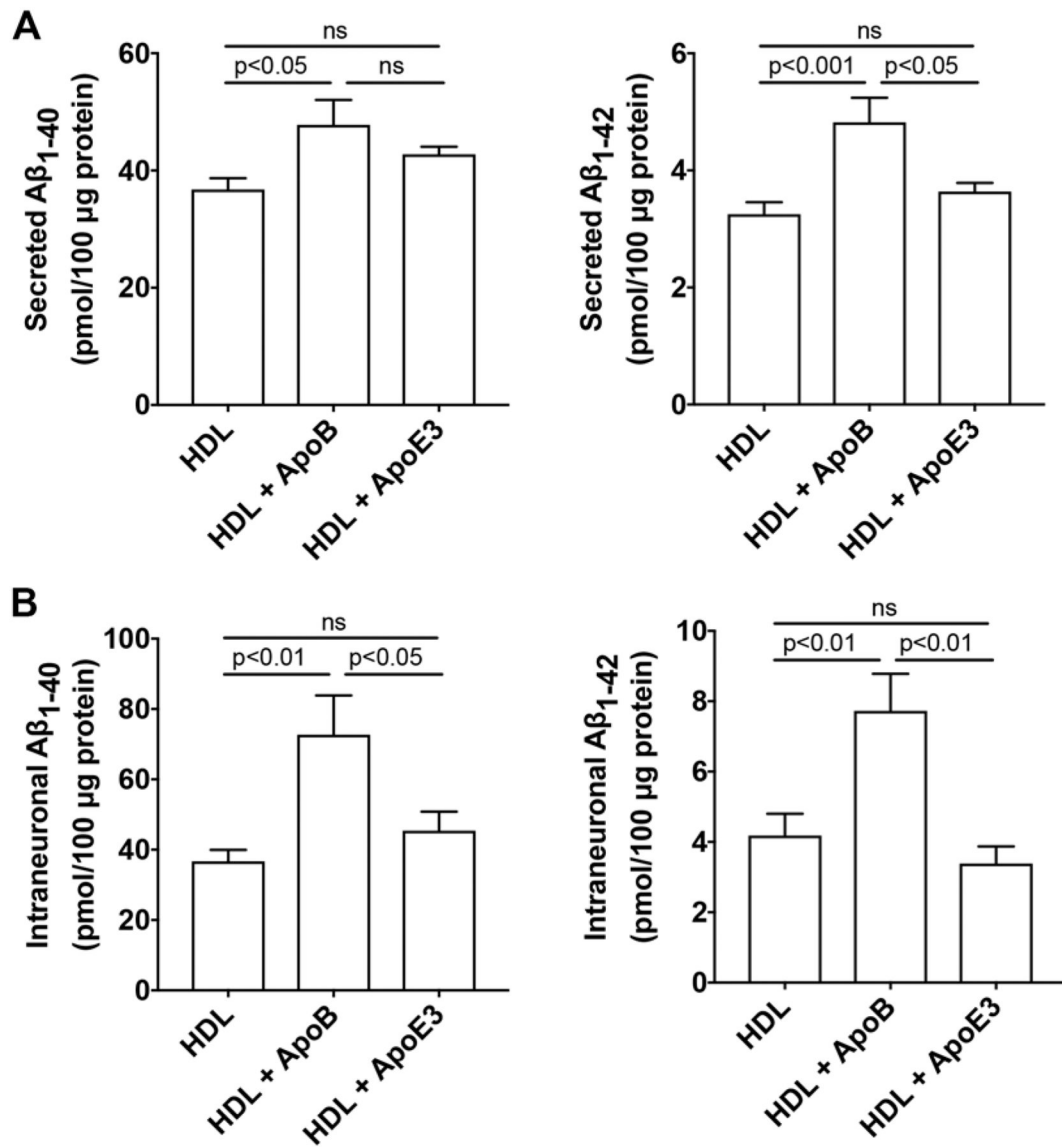


**Figure 2. HDL mixed with apoB, but not HDL mixed with apoE3, increased Aβ.**

(A) In SH-SY5Y cells expressing wild-type AβPP, treatment with HDL (50 μg/ml) mixed with apoB (20 μg/ml) for 3 days significantly increased secreted levels Aβ<sub>1-40</sub> and Aβ<sub>1-42</sub>. Treatment with HDL (50 μg/ml) mixed with apoE3 (20 μg/ml) for 3 days did not significantly increase secreted levels of Aβ (n=5). (B) In SH-SY5Y cells expressing wild-type AβPP, treatment with HDL (50 μg/ml) mixed with apoB (20 μg/ml) for 3 days significantly increased intraneuronal levels of Aβ<sub>1-40</sub> and Aβ<sub>1-42</sub>. Treatment with HDL (50 μg/ml) mixed with apoE3 (20 μg/ml) for 3 days did not significantly increase intraneuronal levels of Aβ (n=5).



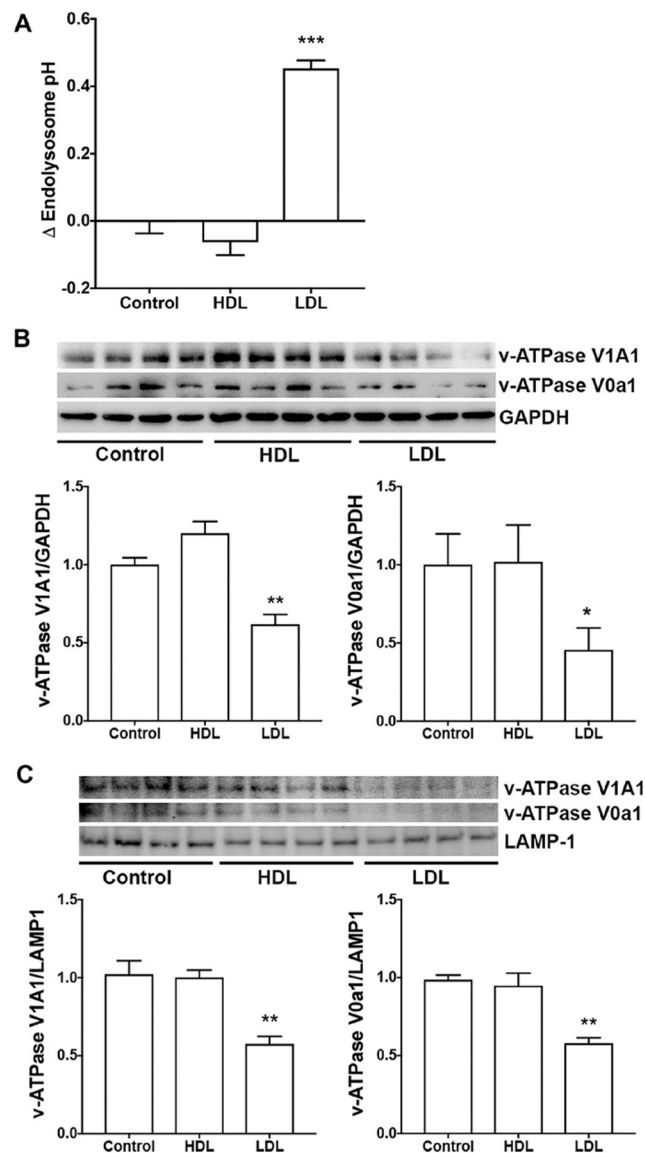


**Figure 3. LDL, but not HDL, de-acidified endolysosomes.**

(A) In SH-SY5Y cells expressing wild-type A $\beta$ PP, LDL (50  $\mu$ g/ml for 3 days), but not HDL (50  $\mu$ g/ml for 3 days), significantly elevated endolysosome pH (\*\*\*) $p < 0.001$ ,  $n = 16$ –20 cells from 4 different plates). (B) LDL, but not HDL, significantly decreased protein levels of V1A1 and V0a1 subunits of v-ATPase in total cell lysates of SH-SY5Y cells (\* $p < 0.05$ , \*\* $p < 0.01$ ,  $n = 4$ ). (C) LDL, but not HDL, significantly decreased protein levels of v-ATPase V1A1 and V0a1 subunits in enriched lysosome fractions of SH-SY5Y cells (\*\* $p < 0.01$ ,  $n = 4$ ).

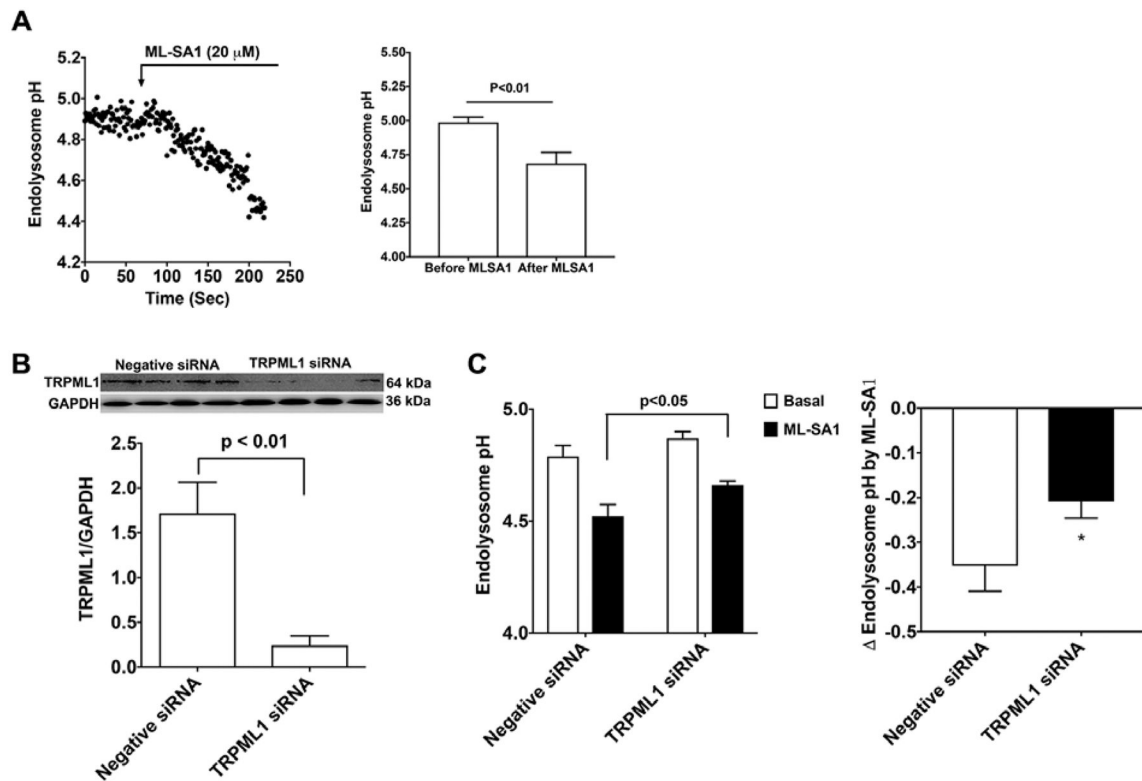


**Figure 4. TRPML1 is involved in ML-SA-induced endolysosome acidification.**

(A) Ratiometric endolysosome pH trace shows the effect of ML-SA1 (20  $\mu$ M) on endolysosome pH in primary cultured rat cortical neurons. Quantified data shows that ML-SA1 (20  $\mu$ M) decreased significantly endolysosome pH (2 min following ML-SA1 treatment vs baseline,  $n=19$  neurons of 4 different plates from two different animals). (B) Immunoblotting shows that TRPML1 siRNA decreased significantly protein levels of TRPML1 in primary cultured neurons ( $n=4$ ). (C) Basal levels of endolysosome pH did not change following treatment with TRPML1 siRNA; however, the magnitude of ML-SA1-induced acidification of endolysosomes (2 min following ML-SA1 treatment) was decreased in TRPML1 siRNA treated neurons when compared with negative siRNA treated neurons ( $*p < 0.05$ ,  $n=15-20$  neurons of 4 different plates from two different animals).

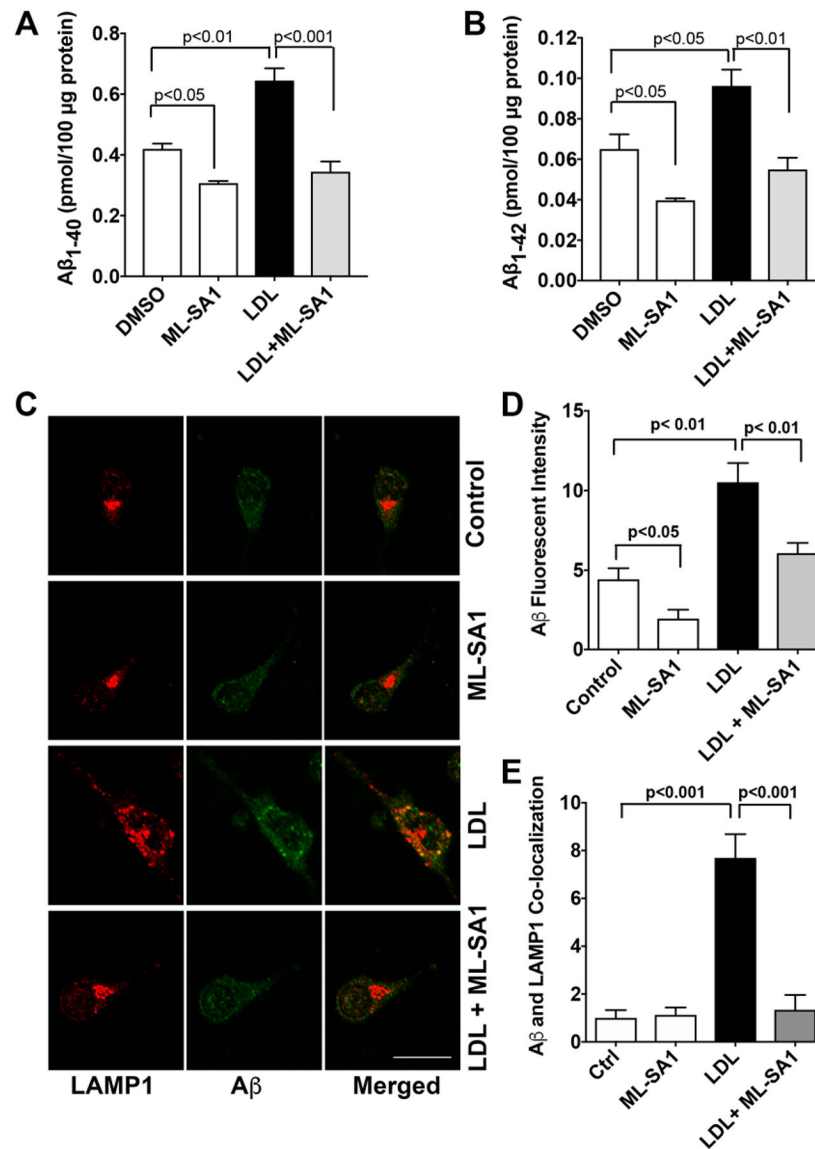


**Figure 5. ML-SA1 prevented LDL-induced increases in Aβ.**

(A, B) LDL (50 μg/ml for 3 days) increased secreted levels of Aβ<sub>1-40</sub> and Aβ<sub>1-42</sub> in primary cultured rat cortical neurons. ML-SA1 treatment (20 μM for 3 days) decreased significantly basal level of secreted Aβ and blocked significantly LDL-induced increases in secreted levels of Aβ<sub>1-40</sub> and Aβ<sub>1-42</sub> (n=4). (C, D) LDL (50 μg/ml for 3 days) increased significantly immunopositive signal of Aβ in primary cultured neurons (Bar = 20 μm, n=15–20 neurons of 4 different plates from two different animals). (E) ML-SA1 (20 μM for 3 days) prevented significantly LDL-induced increased co-localization of Aβ with LAMP1-positive endolysosomes (n=15–20 neurons of 4 different plates from two different animals).

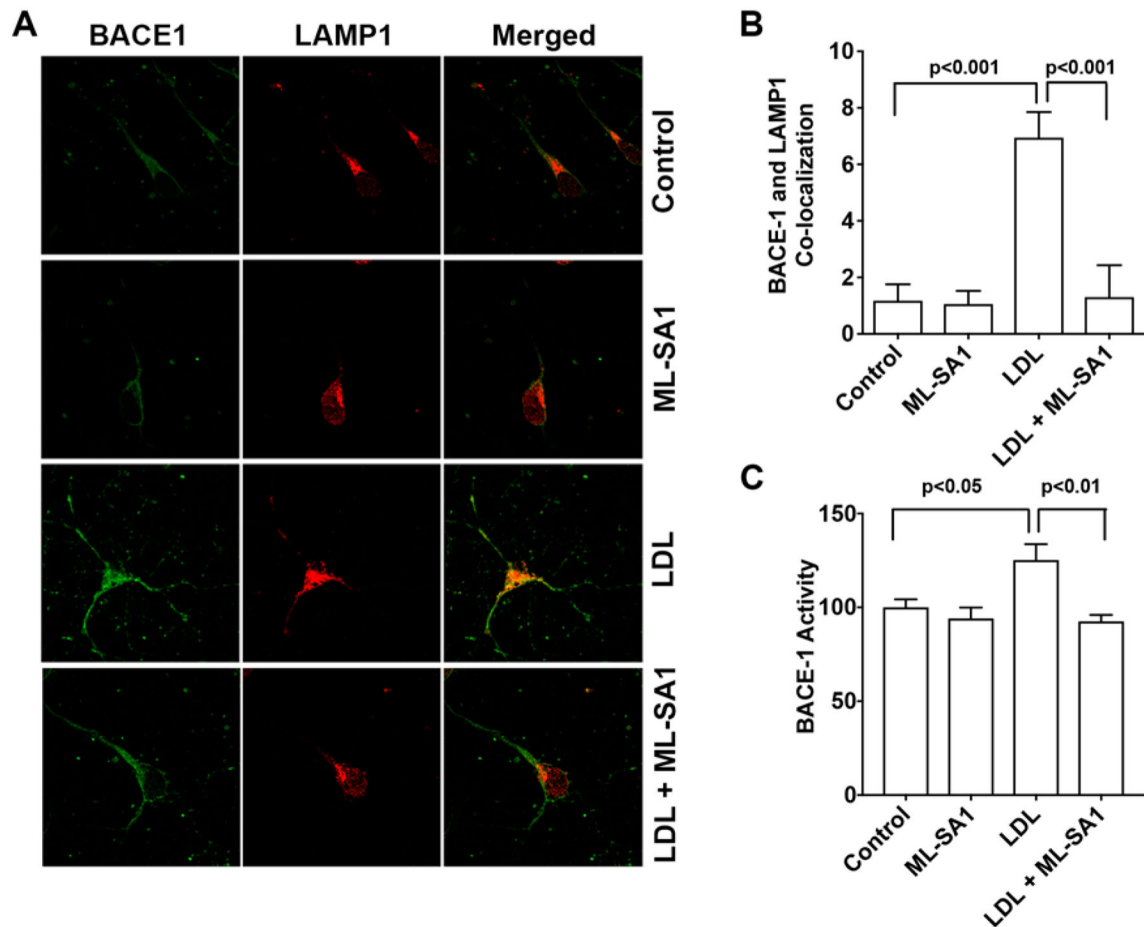


**Figure 6. ML-SA1 prevented LDL-induced increases in the colocalization of BACE1 with LAMP1 and increases in BACE1 enzyme activity.**

(A,B) In primary cultured rat cortical neurons, LDL (50  $\mu\text{g}/\text{ml}$  for 3 days) increased immunopositive signals of BACE1 and the co-localization of BACE-1 with LAMP1 positive endolysosomes, and such effects were prevented by ML-SA1 (20  $\mu\text{M}$ ) co-treatment (n=15–20 cells of 4 different plates from two different animals). (C) In primary cultured rat cortical neurons, LDL (50  $\mu\text{g}/\text{ml}$  for 3 days) increased significantly BACE1 activity, and ML-SA1 (20  $\mu\text{M}$  for 3 days) blocked significantly LDL-induced increases in BACE1 enzyme activity (n=4).

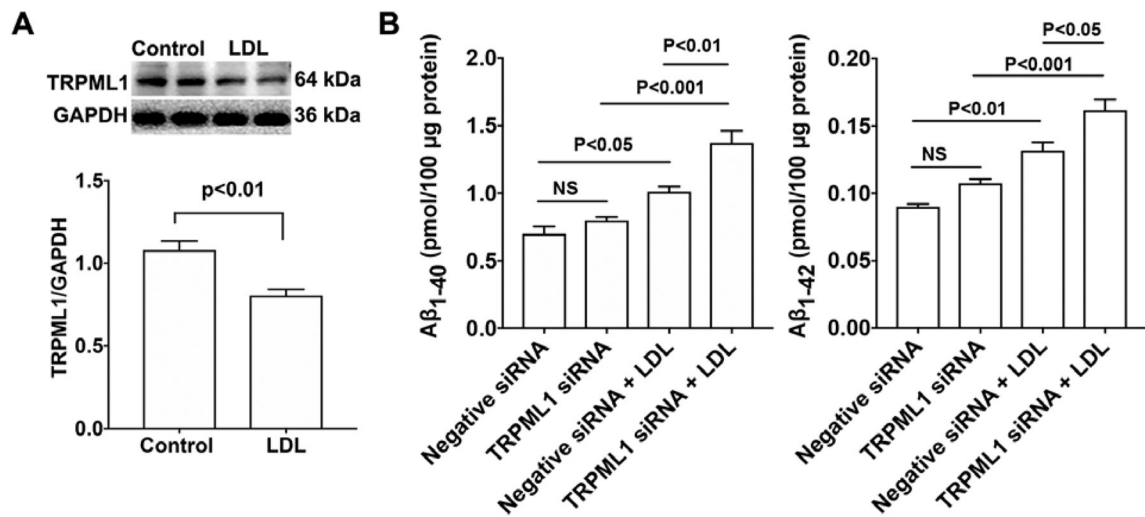


**Figure 7. TRPML1 knockdown potentiated LDL-induced increases in Aβ.**

(A) LDL (50 μg/ml for 3 days) significantly decreased protein levels of TRPML1 in primary cultured rat cortical neurons (n=4). (B) TRPML1 knockdown, *per se*, did not affect secreted Aβ levels. However, TRPML1 knockdown significantly exacerbated LDL-induced increases in Aβ levels in primary cultured rat cortical neurons (n=4).